ADVANCE SPICE MODEL FOR ESD DIODES: ASM-ESD

PRELIMINARY DOCUMENTATION OF ASM-ESD FOR PHASE III

Sourabh Khandelwal
Email: sourabh.khandelwal@mq.edu.au

School of Engineering

Macquarie University

December 2021

Contents

1 Note

This is a short description of ASM-ESD model to support CMC members in phase III. A complete technical manual will be provided in the next phase.

2 Acknowledgements

The authors will like to acknowledge Michi Stockinger (NXP), You Li (Globalfoundries at the time), Meng Miao (Globalfoundries and ESD modeling WG chair), Prabhu (Globalfoundries) and Paul Zhou (Analog Devices) for helpful discussions and feedback on numerous ocassions during the model development. The authors would also like to thank CMC members supporting this model.

3 Introduction

Gummel-Poon model formulations have been enhanced significantly to model the specific features pertinent to ESD simulations to develop ASM-ESD compact model. In several cases new physics-based formulation have been developed to cover all the features needed for an accurate ESD diode compact model. Following sections describe the model topology, model features, formulations, and model parameters to model the various aspects of ESD diode modeling. The model is developed in CMC standard Verilog-A programming language. CMC recommended Verilog-A coding practices have been followed in the development of the model code.

4 Model Topology

ASM-ESD model is four terminal model with collector (C), and base (B), and emitter (E) as the three electrical terminals, and a thermal node (DT) as the fourth terminal. DT can be used to connect external thermal networks with appropriate setting of self-heating model. Model topology is shown in Fig. 1.

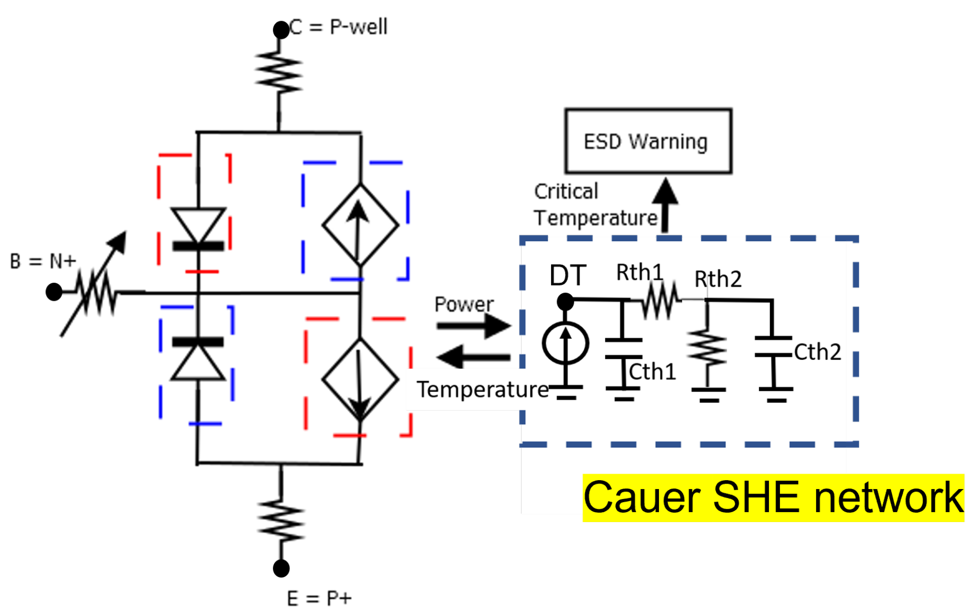

Figure 1: ASM-ESD diode model topology. C represents substrate connection in a diode, B and E represent the anode or cathode of the diode.

5 Model features and parameters

5.1 I-V model parameters

I-V model results achieved during phase II are shown in Fig. 2. The model parameters exercised for these I-V model results are:

- Forward I-V parameters: IS, NF, RB, RE, RC.
- Reverse I-V parameters: ISATR, VTR, NTR.
- Temperature dependence parameters: XTI, XTIR.

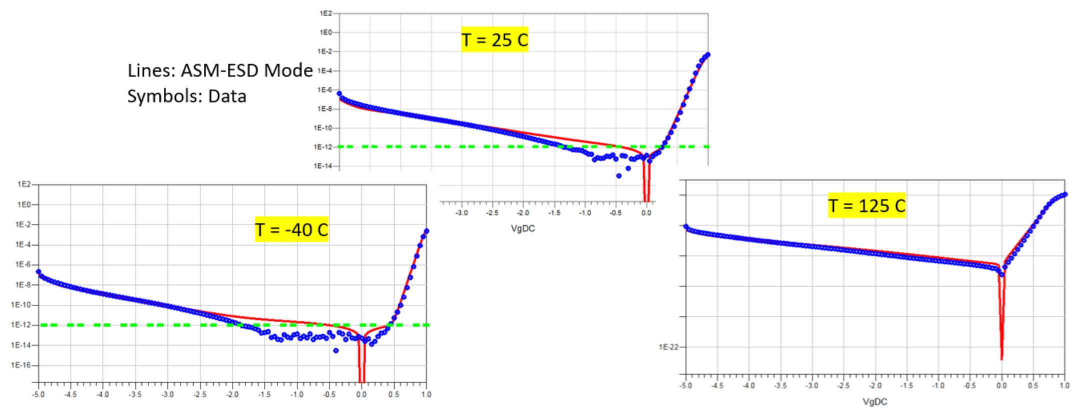

Figure 2: Forward and reverse I-V model results.

5.2 C-V model parameters

The model parameters exercised for C-V model shown in Fig. 3 are: CJE, VJE, and MJE.

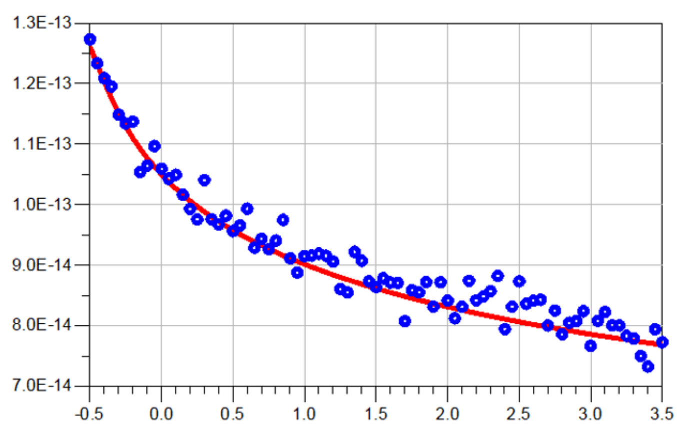

Figure 3: C-V model results.

5.3 Post breakdown resistance model parameters

The model parameter exercised for modeling the resistance of the diode after the reverse breakdown are: IJBV, THER, THEREXP. Temperature dependence of post reverse breakdown model XJBV, XTHEEXP, and XBVR have been used to model temperature dependence of this behavior.

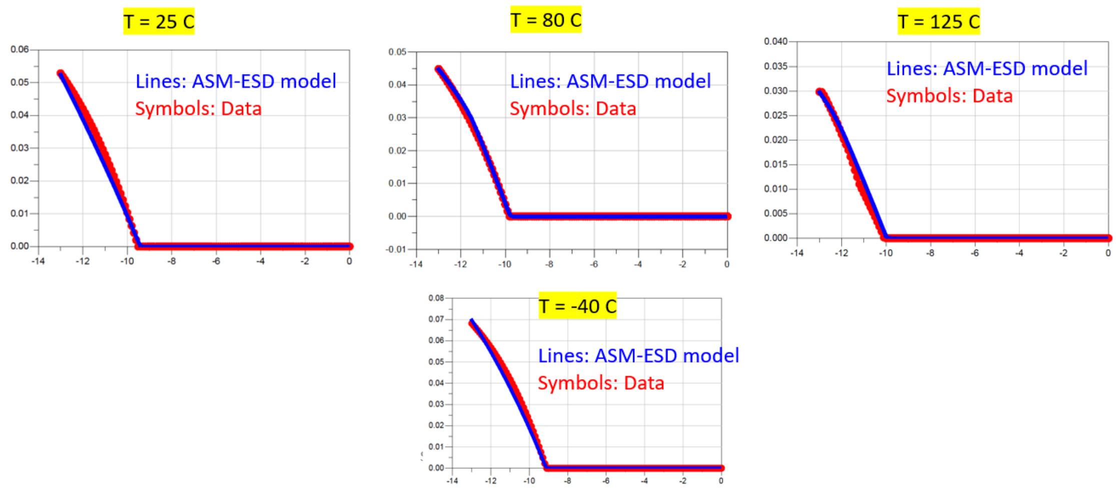

Figure 4: Post reverse breakdown resistance model results.

5.4 Overshoot model parameters

To model the overshoot effects following parameters can be exercised:

- Transit time parameters: TF, ATFF, VTF0, and TEXP.
- Base resistance parameters: RB, VTT0, VSATB.

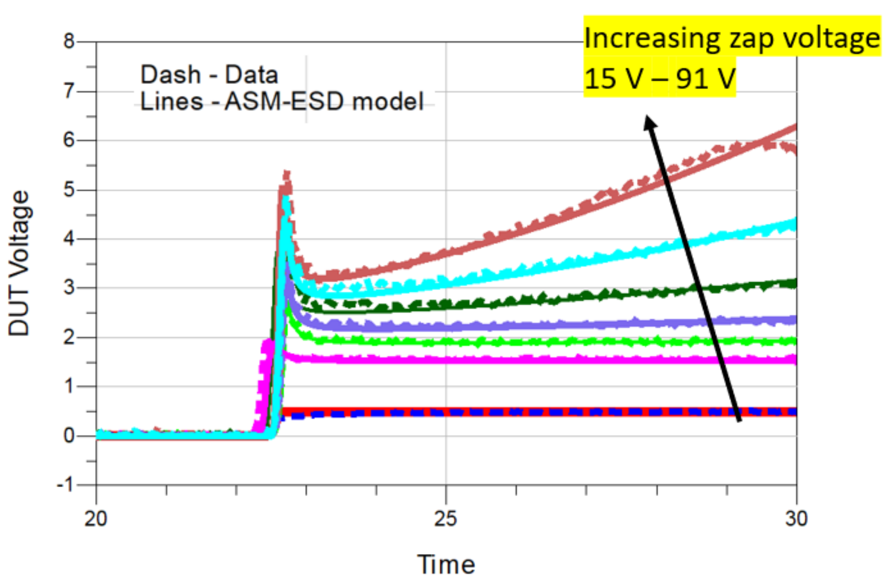

Figure 5: Overshoot model results.

Beyond the overshoot the self-heating effect seen in the transient data is modeled with the thermal model parameters RTH0, CTH0, RTH1, and CTH1. The parameters modeling the temperature dependence of base-, emitter-, and collector resistances are also used. These are ARB, ARE, and ARC respectively.

5.5 BJT Gain model parameters

The gain of the parasitic BJT is modeled with parameter BF. The roll-off of gain with current is modeled with parameters IKF, VAR, and XKF.

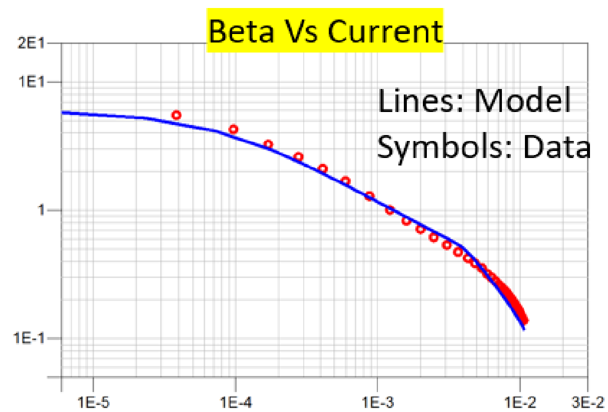

Figure 6: Parasitic BJT model results.

5.6 BJT Gain V_{cb} dependence

Change in BJT gain with V_{cb} is modeled with parameters IKBWM, KBWM, and XBWM.

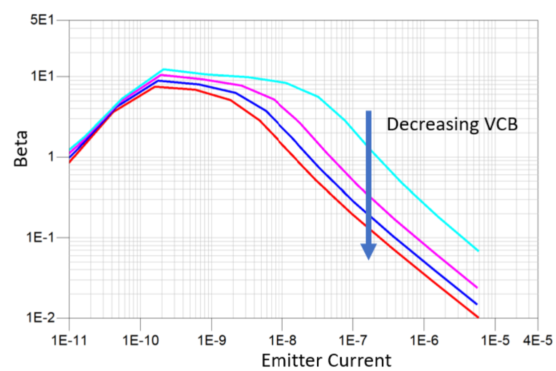

Figure 7: BJT gain V_{cb} dependence.

5.7 Delayed BJT response model parameters

The delayed response of BJT is modeled show in Fig. 8 with a separate time-constant. This is modeled with parameter CTHBB.

6 Model formulations

6.1 Intrinsic voltage

The effect of base-, collector-, and emitter-resistance are subtracted from the externally applied voltages to calculate the intrinsic voltages.

$$V_{b,i} = V_b - I_b \cdot R_b \tag{1}$$

$$V_{c,i} = V_c - I_c \cdot R_c \tag{2}$$

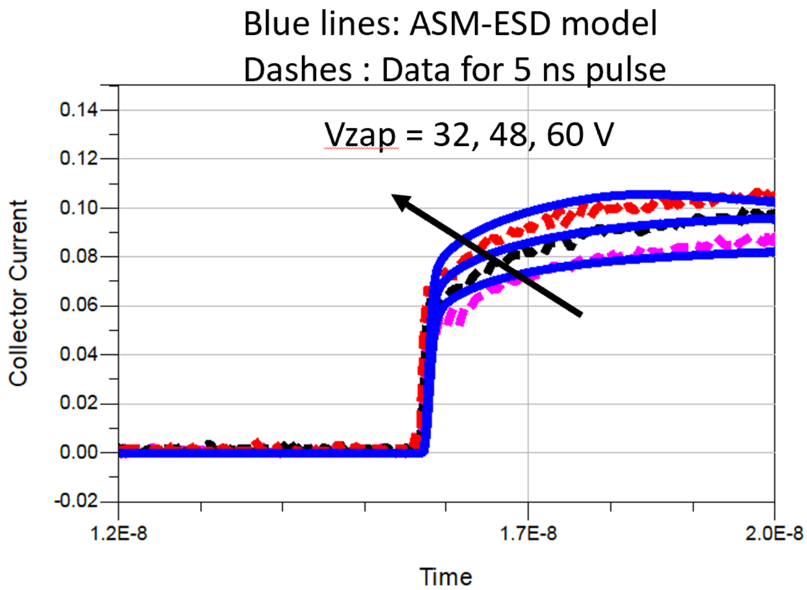

Figure 8: Delayed BJT response model results.

$$V_{e,i} = V_e - I_e \cdot R_e \tag{3}$$
$$V_{be,i} = V_{b,i} - V_{e,i} \tag{4}$$
$$V_{bc,i} = V_{b,i} - V_{c,i} \tag{5}$$

6.2 I-V model formulations

The total emitter current (see Fig. 1) is sum of base, and collector current. Base current I_b is given by,

$$I_b = I_{be} + I_{bc} \tag{6}$$

where I_{be} and I_{bc} are the currents in base-emitter and base-collector junctions respectively. I_{be} is the active current for usual ESD diode operation and modeling. I_b is further formulated as,

$$I_{be} = \frac{I_f}{BF} + I_{be,r} \tag{7}$$
$$I_f = I_1 - I_2 \tag{8}$$
$$I_1 = IS \cdot \left(exp(\frac{V_{be,i}}{NF \cdot V_t}) - 1 \right) \tag{9}$$
$$I_2 = \frac{IJBV}{1 + THER \cdot V_{be,i}^{THEEXP}} \cdot \left(exp(\frac{-V_{be,i} - BV}{NBV \cdot V_t}) - 1 \right) \tag{10}$$

I_f models the forward, reverse breakdown, and post-breakdown behavior of the ESD diode. $I_{BE,r}$ models tunneling and recombination current under the conditions of small reverse bias. It is formulated as,

$$I_{be,r} = ISATR \cdot \left(exp(\frac{-V_{be,i} \cdot VTR}{NTR \cdot V_t \cdot (VTR - V_{be,i})}) - 1 \right) + ISE \cdot \left(exp(\frac{V_{be,i}}{NE \cdot V_t}) - 1 \right) \tag{11}$$

Equivalent to Eqs. 7 - 11 for I_f and $I_{BE,r}$ following formulations exist for base-collector junction current.

$$I_{bc} = \frac{I_r}{BR} + I_{bc,r} \tag{12}$$
$$I_r = I_3 - I_4 \tag{13}$$

$$I_3 = IS \cdot \left(exp(\frac{V_{bc,i}}{NR \cdot V_t}) - 1 \right) \quad (14)$$

$$I_4 = \frac{IJBVC}{1 + THER \cdot V_{bc,i}^{THEEXP}} \cdot \left(exp(\frac{-V_{bc,i} - BVC}{NBVC \cdot V_t}) - 1 \right) \quad (15)$$

$$I_{bc,r} = ISATR \cdot \left(exp(\frac{-V_{bc,i} \cdot VTRC}{NTRC \cdot V_t \cdot (VTRC - V_{bc,i})}) - 1 \right) + ISC \cdot \left(exp(\frac{V_{bc,i}}{NC \cdot V_t}) - 1 \right) \quad (16)$$

The collector current is given by,

$$I_c = I_{tf} - I_{tr} \quad (17)$$

$$I_{tf} = I_f \cdot I_{k1} \quad (18)$$

$$I_{tr} = I_r \cdot I_{k1} \quad (19)$$

$$I_{k1} = 2 \cdot \frac{1 - \frac{V_{be,i}}{VAR} - \frac{V_{bc,i}}{VAF}}{1 + T_0^{XKF}} \quad (20)$$

$$T_0 = 1 + 4 \cdot \frac{I_f}{IKF} + \frac{I_r}{IKR} \quad (21)$$

I_{k1} accounts for the high level injection and BJT gain reduction.

6.3 Base resistance formulations

High field, and the effect of charge modulation is modeled with following formulations.

$$R_b = RB \cdot \frac{1 + T_1^{MEXP}}{1 + T_2^{QEXP}} \quad (22)$$

$$T_1 = 1 + \frac{V_{be,i}}{VSATB} \quad (23)$$

$$T_2 = 1 + \frac{Q_m}{VTT0} \quad (24)$$

Q_m is obtained by solving the differential equation Eq. 25 in the model.

$$\frac{dQ_m}{dt} + \frac{Q_m}{T_f} - I_f = 0 \quad (25)$$

The effect of mobility degradation under the influence of high-field on transit time (T_f) is modeled with,

$$T_f = \frac{L_p^2}{D} \quad (26)$$

where L_p is the length, and D is the diffusion constant. Considering the relationship between D and mobility to be,

$$D = \mu_{eff} \frac{kT}{q} \quad (27)$$

where μ_{eff} includes the effect of electric field on the mobility with

$$\mu_{eff} = \frac{\mu_0}{1 + (\mu_0 \cdot E/v_{sat})^{TEXP}} \quad (28)$$

To simplify the implementation, the field dependence of transit time due to mobility variation is modeled by combining equations Eq. 26 to Eq. 28 resulting in,

$$T_f = TF \cdot \left(1 + ATFF \cdot (\frac{V_{be,i}}{VTF0})^{TEXP} \right) \quad (29)$$

6.4 Capacitance formulations

The capacitance of the junctions have been implemented with formulation for the junction charges. The junction charge formulations lead to following equations for the space charge and diffusion capacitors.

$$C_{be} = \frac{CJE}{(1-(\frac{V_{be,i}}{VJE})^{MJE}} + \frac{T_f}{NF \cdot V_t} \cdot IS \cdot \left(exp(\frac{V_{be,i}}{NF \cdot V_t}) \right) \tag{30}$$

$$C_{bc} = \frac{CJC}{(1-(\frac{V_{bc,i}}{VJC})^{MJC}} + \frac{T_r}{NR \cdot V_t} \cdot IS \cdot \left(exp(\frac{V_{bc,i}}{NR \cdot V_t}) \right) \tag{31}$$

6.5 Self-heating effect

A second order Cauer network is implemented in the model for self-heating effect. The thermal network parameters include RTH0, CTH0, RTH1, and CTH1.

6.6 Temperature dependence

Ambient temperature T dependence of all key parameters have been implemented with following formulations. Device temperature T_{dev} is obtained by,

$$T_{dev} = T + \Delta T \tag{32}$$

where ΔT is temperature rise due to the self-heating effect.

$$\rho_t = \frac{T_{dev}}{TNOM} \tag{33}$$

$$LR_t = ln(\rho_t) \tag{34}$$

$$A_t = XTI \cdot LR_t + E_g \cdot (\rho_t - 1) \tag{35}$$

$$Ar_t = XTIR \cdot LR_t + E_g \cdot (\rho_t - 1) \tag{36}$$

$$Is_t = IS \cdot exp(A_t) \tag{37}$$

$$IsR_t = ISR \cdot exp(Ar_t) \tag{38}$$

$$IJBV_t = IJBV \cdot (1 + XJBV \cdot (\rho_t - 1)) \tag{39}$$

$$BVR_t = BVR \cdot (1 + XBVR \cdot (\rho_t - 1)) \tag{40}$$

$$THEEXP_t = THEEXP \cdot (1 + XTHEEXP \cdot (\rho_t - 1)) \tag{41}$$

$$BF_t = BF \cdot exp(XTB \cdot LR_t) \tag{42}$$

Temperature dependence of base-, collector-, and emitter resistances is modeled with,

$$RB_t = RB \cdot \rho_t^{ARB} \tag{43}$$

$$RC_t = RC \cdot \rho_t^{ARC} \tag{44}$$

$$RE_t = RE \cdot \rho_t^{ARE} \tag{45}$$